IEEE Open Journal of the Communications Society

Received 7 August 2020; revised 25 August 2020; accepted 26 August 2020. Date of publication 2 September 2020; date of current version 18 September 2020.

Digital Object Identifier 10.1109/OJCOMS.2020.3021129

Throughput and Delay Analysis of IEEE 802.11-Based Tree-Topology Networks

TAKESHI KANEMATSU[1] (Member, IEEE), YIN WAN[1], KOSUKE SANADA[2] (Member, IEEE), ZHETAO LI[3] (Member, IEEE), TINGRUI PEI[3], YOUNG-JUNE CHOI[4] (Senior Member, IEEE), KIEN NGUYEN[1] (Senior Member, IEEE), AND HIROO SEKIYA[1] (Senior Member, IEEE)

[1]Graduate School of Engineering, Chiba University, Chiba 263-8522, Japan

[2]Mie University, Mie 514-8507, Japan

[3]Xiangtan University, Xiangtan 411105, China

[4]Ajou University, Suwon 16499, South Korea

CORRESPONDING AUTHORS: K. NGUYEN AND H. SEKIYA (e-mail: nguyen@chiba-u.jp; sekiya@faculty.chiba-u.jp)

This work was supported by JSPS KAKENHI under Grant 19K20251 and Grant 20H04174. The work of Kien Nguyen was supported by the Leading Initiative for Excellent Young Researchers (LEADER) Program from MEXT, Japan.

ABSTRACT This article aims to investigate the performance of the IEEE 802.11-based tree-topology network, where a wireless node is within the others' carrier sensing ranges. In such a network, the concurrent transmission is a dominant cause of frame collisions. Moreover, the relay nodes (RN) (i.e., in the tree) likely cause the coexistence of non-saturated and saturated nodes in the networks. Those conditions have not been addressed in the previous works yet. As a solution, this work proposes new analytical expressions of delay and throughput in the investigated scenario. The presented analytical model incorporates the Bianchi model and airtime concept to formulate operations of the IEEE 802.11 nodes. First, by leveraging Bianchi-based analysis, the proposed model gives the frame collision probability caused by concurrent transmission. Second, by using airtime concept analysis, the ratio of frame numbers of each flow in a relay node (RN) is expressed to represent the buffer state of RN. As a result, we can obtain the network throughput, the throughput, and the delay of each flow. The validity of the analytical expressions is confirmed by the quantitative agreement between the analytical and simulation results.

INDEX TERMS Tree topology, performance analysis, airtime, Bianchi, throughput, delay.

I. INTRODUCTION

THE IEEE 802.11 technology and its variants have been hugely successful with a wide range of applications ranging from daily Internet access to vehicle-to-vehicle communication [1]–[3], environmental monitoring [4], [5], etc. Typically, the technology appears in the form of Wireless Local Area Networks (WLANs) with either single-hop or multi-hop deployments. While we can see the former almost everywhere (i.e., Wi-Fi networks), the latter is gaining more popularity due to its usefulness and applicability. For example, the multi-hop IEEE 802.11-based networks can serve as a disaster-resilient network to provide quick Internet connection in the afflicted area [6]–[8] or agricultural control [9]. In such networks, the routing protocols, which guarantee efficient upward and downward communications at each node, are often expected to be simple. As a result, the routing protocols mostly formulate a tree-topology in the multi-hop IEEE 802.11 networks. In such a context, it is essential and valuable to establish mathematical models for network performance. Among the other theories, the Bianchi model and the airtime analysis are the most popular ones for understanding the WLAN performance.

The Bianchi model is considerably canonical for WLAN analysis [10], in which the IEEE 802.11 backoff timer (BT) decrement is modeled by a Markov chain. The model hence reveals the transmission probability when the node is in the BT-decrement period. Moreover, with the transmission probability, it is possible to give a concurrent transmission collision probability with nodes in the carrier-sensing range (e.g., of a WLAN). Since the Bianchi model appeared,

it has established a solid foundation for many improvements [11]–[17], such as those relating to a generalized expression in saturation conditions [11], non-saturation conditions [13], the impacts of Request to Send/Clear to Send (RTS/CTS) [14], etc. However, using the Bianchi-like models, it is not straightforward to express network performance in several varying conditions such as different packet sizes. Besides, it is challenging for the models to handle the WLAN that has a mix of saturated and non-saturated nodes. Those conditions are inherently popular in the tree-based IEEE 802.11 network.

The airtime concept, which is original in [18], has been a root of many existing works in understanding the performance of IEEE 802.11 networks [19]–[32]. In the airtime-based analysis, the airtime parameters represent intervals occupied by the states of a wireless node. Moreover, it can reveal the time overlap of different states among several nodes of a WLAN, for example, expressions of hidden-node frame collisions or carrier sensing states. As a result, in the multi-hop WLAN, the channel access situations of nodes can be expressed as simple functions of airtime. The airtime analysis is successful when handling various IEEE 802.11 characteristics, such as coupling effects [25], capture effects [32], etc. However, the previous works mostly focus on the string topology without considering the conditions as mentioned above. The recent work in [16] shed light on the feasibility of using airtime to analyze the single-hop WLAN with the mixed types of nodes under varying packet sizes. In an IEEE 802.11 tree-topology network, relay nodes (RNs) relay multiple flows, each of which is similar to a string IEEE 802.11 network with varying traffic patterns. That suggests that the airtime concept might be useful for performance analysis of the tree-topology networks.

This article presents analytical expressions of delay and throughput for tree-topology networks, where all nodes are within the others' carrier sensing ranges, with a consideration of varying offered loads. In the investigated scenario, the traffic patterns are the upstream flows from the leaves to the root in a three-layer tree. In such IEEE 802.11-based tree-topology network, concurrent transmissions are the dominant cause of frame collisions since nodes sense each other's communications. Moreover, the relay nodes, which receive packets from the leaves and forward to the root, may make networks in a mixed condition with unsaturated and saturated nodes. The presented analytical model newly formulates relay-node operations by incorporating the Bianchi model with the airtime analysis. While the former is adopted to express the frame collision probability caused by concurrent transmission, the latter is used for revealing the ratio of frame numbers of each flow in a relay node (RN). As a result, we have successfully obtained each flow's performance (i.e., including throughput and delay) and network throughput. The validity of the analytical expressions is confirmed by the quantitative agreement between the analytical and simulation results.

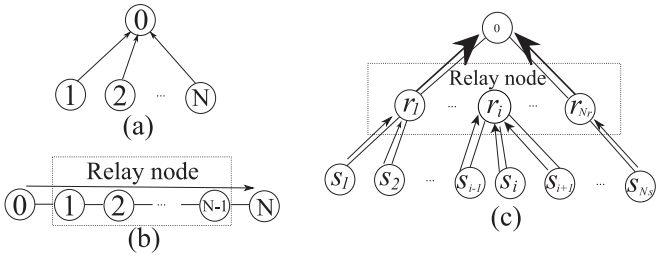

FIGURE 1. Examples of WLAN's network topologies (0: destination node); (a) Star topology (b) String topology with $(N+1)$ nodes (c) Tree topology with N_R relay nodes and N_S source nodes.

The rest of the paper is organized as follows. The next section introduces the related works. Section III presents our approach for throughput and delay analysis. In Section IV, the analytical results are compared to the simulation ones. Finally, Section V concludes the paper and introduces future works.

II. RELATED WORKS

Figure 1 shows examples of typical WLAN topologies, including star, string, and tree topology. There are many analytical models for the single hop or the star topology (i.e., as depicted in Fig. 1(a)) [10]–[17]. Most of the works have relied on the Bianchi model [10], which can express the BT decrement resulting in the expression of 802.11 node's operation in each time slot. The model has been continuously applied to understand wireless networks' performance and behaviors, including advanced IEEE 802.11 standard, such as 802.11ac [33]. The work in [11], which investigates the Bianchi model's fixed-point formulation, provides an explicit expression for WLAN performance metrics. In [14], the authors have improved the model to include overhead causing by the RTS/CTS handshake. However, similar to the Bianchi model, those works assume that all network nodes are in saturation conditions. In [12], [13], the authors have extended the Bianchi model to the WLANs, which have heterogeneous and unsaturated conditions. The model can predict the peak throughput in the WLAN before reaching the saturation condition. Saturation and non-saturation nodes can coexist in the tree-topology networks, but it is generally difficult to account for both the types of nodes in Bianchi's model-based analyses.

Regarding the string topology WLAN as in Fig. 1(b), there is a large amount of article in theory aiming to analyze the network performance [18]–[32]. One of the most effective approaches to analyze such multi-hop network is employing the airtime concept. With the concept, at each node in the network, different airtime parameters are defined following the states of network node during an operational time [18]. In [18], the authors could obtain the saturated throughput of a string topology network with a sufficient hop number. The work in [22] extended the airtime concept to model the two-way flow for Voice over Internet Protocol (VoIP) traffic. In [23], [24], the authors have respectively quantified the throughput of a multi-hop network with

RTS/CTS considerations and long frames using the concept. The model 's applicability has also been found in WLANs with coupling effect [25], capture effect [34], or WLANs with internetwork-interferences [35]. Additionally, the analysis can well express different environments, such as 802.11e Enhanced Distributed Channel Access (EDCA) multi-hop networks [27], ad-hoc multi-channel networks [30], multi-hop networks considering multi-rate [32], and 802.11p EDCA WLANs [17]. The airtime concept has generalized analytical expressions for string-topology multi-hop networks [31]. Using the concept also can express the coexistence states of saturation and non-saturation nodes [16], [26]. However, most of the proposed models are for either the star topology or the string topology with the single-flow.

In a tree-topology network depicted in Fig. 1(c), Relay nodes may relay multiple flows. Therefore, the network operation becomes very different compared to the string topology. In [16], the authors have introduced the airtime-based model for the WLAN analysis considering multiple flows. The models can express both the throughput of saturation and non-saturation nodes. Moreover, the throughput of multiple flows with different frame lengths can be determined. However, in the analysis model, there are no relay nodes in the network. Hence, it can not be directly applicable to the tree-topology network. Addressing the shortcomings of previous works, we aim to achieve performance analysis for the WLAN with tree-topology. Our analytical models will handle the cases with multiple traffic flows at the RNs, which have different frame lengths. Note that, besides using the airtime concept, there is a related work, which takes a different approach [36], addressing a similar scenario and traffic patterns. In that work, the authors perform the analysis relying on the link characteristic. Meanwhile, our work reckons on the node characteristic. Moreover, they assume the carrier sensing is instantaneous (i.e., propagation delay + carrier sense delay = 0). On the other hand, we need the assumption of all nodes within their carrier sensing ranges, aiming to characterize the effect of carrier sense using airtime.

III. THROUGHPUT AND DELAY ANALYSIS

This work investigates the IEEE 802.11-based tree-topology network, as shown in Fig. 1(c). Each source node (SN) transmits frames to the destination node through relay nodes (RNs). We aim to derive analytical expressions of delay and throughput at any offered load. The following analysis is based on the below assumptions.

1) SNs generate User Datagram Protocol (UDP) frames with constant occurrence probabilities, which follow a Poisson distribution.
2) RNs never generate transmission frames by themselves and only relay frames to the destination.
3) All the network nodes are in the carrier-sensing range one another. There are no nodes hidden from all the other nodes.

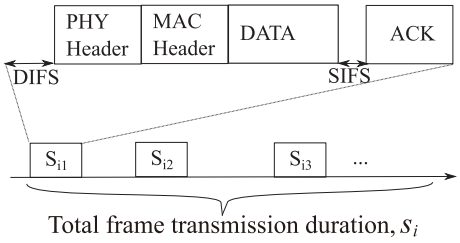

FIGURE 2. Example of transmission airtime.

4) The channel condition is ideal. Therefore, transmission failures occur due to frame collisions in the Medium Access Control (MAC) layer.

By expressing the frame-existence and transmission probabilities of SNs and RNs, the presented analytical model reveals the buffer states of RNs. For obtaining the throughput and delay, transmission airtimes, collision probabilities, frame-existence probabilities, transmission probabilities, carrier-sensing airtimes, and idle airtimes are expressed with respect to each node. Before going into the detailed analysis, we summarize the used notations in Table 1.

A. TRANSMISSION AIRTIME

The transmission airtime of Node i, denoted as X_i, is the timeshare for frame transmission at the node during an operation period. X_i includes the duration of both the successful and failure transmissions [18]. The value of X_i is defined as

$$X_i = \lim_{Time \to \infty} \frac{s_i}{Time}, \tag{1}$$

where $Time$ is the total operation period; s_i is the sum of the durations of the data-frame transmissions ($DATA$), ACK frame-transmissions (ACK), Distributed InterFrame Space ($DIFS$), and Short InterFrame Space ($SIFS$). Figure 2 illustrates an example of transmission airtime.

B. FRAME-COLLISION PROBABILITY

Following assumption 3, a frame collision occurs when the BTs of multiple nodes become zero simultaneously. We denote the transmission probability of Node i in the channel idle state as τ_i. Then the collision probability for a frame transmitted by Node i, γ_i, is

$$\gamma_i = 1 - \prod_{\substack{j \in \boldsymbol{S} \\ j \neq i}} (1 - \tau_j) \prod_{\substack{k \in \boldsymbol{R} \\ k \neq i}} (1 - \tau_k), \tag{2}$$

where $\boldsymbol{S}$ and $\boldsymbol{R}$ are the set of SNs and RNs, respectively.

C. FRAME-EXISTENCE PROBABILITY OF SN

From Assumption 1, SNs generate frames with constant occurrence probabilities. The frame-existence probability of SN i in the non-saturation condition, q_i', is expressed as

$$q_i' = \frac{\lambda_i V_i \sigma}{Z_i}, \tag{3}$$

TABLE 1. Notation used in this work.

Notation	Description
s_i	total transmission duration at Node i in $[0, Time]$
X_i	transmission airtime of Node i
Y_i	carrier-sensing airtime of Node i
Z_i	idle airtime of Node i
τ_i	frame transmission probability at the idle state of Node i
γ_i	frame-collision probability of at Node i
$\boldsymbol{S}$, $\boldsymbol{R}$	set of SNs and RNs
$q_i^{'}$	frame-existence probability of Node i in the non-saturation condition
q_i	frame-existence probability of Node i
λ_i	frame occurrence rate in Node i
O_i	offered load at Node i
P_i	Data payload size at Node i
e_i	Node i's throughput
T_i	needed period of a successful data transmission of Node i
$q_{i,j}$	frame-existence probability of RN i that has a frame from SN j
G_i	transmission probability of Node i being in the idle state under the saturation condition
R_i	mean number of frame transmission attempts
V_i	BT-decrement for successful transmission of one frame at Node i
CW_{min}, CW_{max}	the minimum, maximum values of contention-window
σ	slot time
$\boldsymbol{N_i}$	set of all nodes except Node i
$\mathfrak{P}(\boldsymbol{N_i})$	power set of $\boldsymbol{N_i}$ covering all transmission patterns
f	number of frame length existing on the network
t_i	time needed for the i-th largest frame transmission
$\alpha_{i,j}$	probability that Node i and the nodes with the j-th largest frame don't collide
$\Lambda_{i,j}$	ratio of the j-th largest frames to all frames received by RN i
$\nu_j(i)$	set of nodes connected to RN i with the j-th largest frame
$E_{i,j}$	SN i the end-to-end throughput of SN i connecting to RN j
Q_i	frame-existence probability at Node i
D_{M_i}	MAC access delay at Node i
μ_i	frame service rate at Node i
ρ_i	buffer-utilization rate at Node i
$b_{i,l}$	probability that Node i has l frames in its buffer
D_{Q_i}	queuing delay of Node i
L	buffer length
D_i	transmission delay of Node i
$D_{i,j}$	end-to-end delay from SN i, which connects to RN j

where λ_i is the frame occurrence rate; $V_i\sigma$ means the average time of BT decrement for the successful transmission of one frame; and Z_i is the idle airtime. The frame occurrence rate of SN i is given by

$$\lambda_i = \frac{O_i}{P_i}, \tag{4}$$

where O_i and P_i are the offered load, data payload size of SN i. Because the frame-existence probability should not be larger than one (i.e., the probability value in the case of saturation), the frame-existence probability q_i of SN i for both non-saturation and saturation cases is

$$q_i = \min\left(1, q_i^{'}\right) = \min\left(1, \frac{\lambda_i V_i \sigma}{Z_i}\right). \tag{5}$$

D. FRAME-EXISTENCE PROBABILITY OF RN

From assumption 2, RNs have frames that are generated from SNs. Figure 3 shows an example of the buffer state of the relay node r_1. The relay node relays frames from four source nodes (i.e., S_1, S_2, S_3, S_4) to the destination node 0. The probability that RN i has a frame from SN j is

$$q_{i,j} = \frac{\frac{e_j}{P_j} V_i \sigma}{Z_i}, \tag{6}$$

where e_j is the throughput from SN j to the RN. e_j is determined as below.

$$e_j = X_j\left(1 - \gamma_j\right)\frac{P_j}{T_j}, \tag{7}$$

where T_j is the time needed for one frame transmission at Node j. Depending on the role of Node i, T_i is expressed as

$$T_i = \begin{cases} DIFS + DATA_i + SIFS + ACK & (i \in \boldsymbol{S}) \\ \frac{\sum_{j \in \nu(i)} q_{i,j} T_j}{\sum_{k \in \nu(i)} q_{i,k}} & (i \in \boldsymbol{R}), \end{cases} \tag{8}$$

where $\nu(i)$ is the set of nodes, which connect to RN i.

Because the frame-existence probability of RN i, q_i, is equal to the total number of receiving frames from SNs, we have

$$q_i = \min\left(1, \sum_{j \in \nu(i)} q_{i,j}\right) = \min\left(1, \sum_{j \in \nu(i)} \frac{\frac{e_j}{P_j} V_i \sigma}{Z_i}\right). \tag{9}$$

E. TRANSMISSION PROBABILITY

According to [11], the frame transmission probability when Node i is in the idle state in the saturation condition (i.e., G_i)

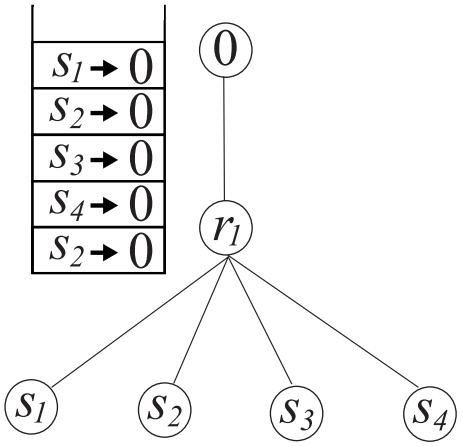

FIGURE 3. Example of relay-node buffer state.

is calculated as follows.

$$G_i = \frac{R_i}{V_i} = \frac{\sum_{s=0}^{K} \gamma_i^s}{\sum_{s=0}^{K} \frac{\gamma_i^s B_s}{2}}, \tag{10}$$

where R_i and V_i are the mean number of frame transmission attempts and BT decrement for the successful transmission of one frame, respectively. The expected value of initial BT for s-th frame retransmission, B_s, is determined in (11).

$$B_s = \begin{cases} 2^s(CW_{min}+1)-1 & (0 \le s \le K'-1) \\ CW_{max} & (K' \le s \le K), \end{cases} \tag{11}$$

where CW_{min} and CW_{max} are the minimum and maximum contention-window values respectively. $K' = \log_2 \frac{CW_{max}+1}{CW_{min}+1}$, and K is the retransmission limit number. In addition, from [19], the relationship between the transmission and idle airtimes in the saturation condition is

$$X_i = \frac{q_i Z_i G_i T_i}{\sigma}, \tag{12}$$

where σ is the slot time.

The general expression of the frame transmission probability of Node i at the channel idle state can be obtained from Eqs. (3), (9), and (10) as

$$\tau_i = q_i G_i. \tag{13}$$

F. CARRIER-SENSING AIRTIME

The carrier-sensing airtime is the timeshare, during which a node has the carrier-sensing state, in the operation period. Besides, the carrier-sensing airtime of Node i, Y_i, is the total transmission airtime of the neighbor nodes within Node i's carrier-sensing range. Using the carrier-sensing airtime makes it possible to express the carrier-sensing state at different length frames.

1) CALCULATION BASED ON ALL TRANSMISSION PATTERNS

The overlaps of the multiple transmissions due to the frame collisions among other nodes must be considered. One simple way to formulate the carrier-sensing airtime taking into account the overlaps is to calculate all transmission patterns. In this method, the carrier-sensing airtime of Node i is

$$Y_i = \frac{Z_i}{\sigma} \cdot \sum_{\boldsymbol{h} \in \mathfrak{P}(\boldsymbol{N_i})} \Bigg[(1-\tau_i) \prod_{j \in \boldsymbol{h}} \tau_j \prod_{\substack{k \notin \boldsymbol{h} \\ k \neq i}} (1-\tau_k) \max_{l \in \boldsymbol{h}} (T_l) + \tau_i \prod_{j \in \boldsymbol{h}} \tau_j \prod_{\substack{k \notin \boldsymbol{h} \\ k \neq i}} (1-\tau_k) F\Big(\max_{l \in \boldsymbol{h}} (T_l) - T_i \Big) \Bigg], \tag{14}$$

where $\boldsymbol{N_i}$ is the set of all network nodes except Node i and $\mathfrak{P}(\boldsymbol{N_i})$ is the power set of $\boldsymbol{N_i}$, which covers all transmission patterns. Additionally, $F(x)$ is determined in (15).

$$F(x) = \begin{cases} x & (x \ge 0) \\ 0 & (x < 0). \end{cases} \tag{15}$$

2) CALCULATION BASED ON FRAME LENGTH

Because Eq. (14) calculates all transmission patterns, the calculation cost increases explosively along with the number of network nodes. It may make the merit of using analytical models, which need low calculation costs, disappear. To reduce the calculation cost, the calculation method based on frame length is proposed. The carrier-sensing time depends on the transmitted frame with the longest transmission time. Therefore, the carrier-sensing airtime is obtained by checking from the nodes, which have larger frames, to the nodes, which have smaller ones. The carrier-sensing airtime of Node i is

$$Y_i = \frac{Z_i}{\sigma} \cdot \begin{cases} \sum_{j=1}^{f} \Big\{ \alpha_{i,1}\alpha_{i,2}\cdots\alpha_{i,j-1}\big(1-\alpha_{i,j}\big) \Big[(1-\tau_i)t_j + \tau_i F\big(t_j - T_i\big) \Big] \Big\} & (i \in \boldsymbol{S}) \\ \sum_{j=1}^{f} \Big\{ \alpha_{i,1}\alpha_{i,2}\cdots\alpha_{i,j-1}\big(1-\alpha_{i,j}\big) \Big[(1-\tau_i)t_j + \tau_i \sum_{k=j+1}^{f} \Lambda_{i,k}\big(t_j - t_k\big) \Big] \Big\} & (i \in \boldsymbol{R}), \end{cases} \tag{16}$$

where f is the number of frame length existing on the network; t_i is the time needed for the i-th largest frame transmission; $\alpha_{i,j}$ is the probability that Node i does not collide with the nodes with the j-th largest frame on the network. $\alpha_{i,j}$ is expressed as follows.

$$\alpha_{i,j} = \prod_{\substack{k \in \boldsymbol{S_j} \\ k \neq i}} (1-\tau_k) \prod_{\substack{l \in \boldsymbol{R} \\ l \neq i}} \big(1 - \tau_l \Lambda_{l,j}\big), \tag{17}$$

where $\boldsymbol{S_i}$ is the set of SNs with the i-th largest frame; $\Lambda_{i,j}$ is the ratio of the j-th largest frames to all frames received by RN i. It is determined as (18).

$$\Lambda_{i,j} = \frac{\sum_{m \in \nu_j(i)} q_{i,m}}{\sum_{n \in \nu(i)} q_{i,n}}, \tag{18}$$

where $\nu_j(i)$ is the set of nodes with the j-th largest frame, which connect to RN i.

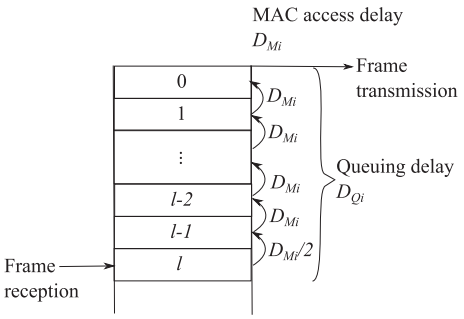

FIGURE 4. Delay constitution.

By using these expressions, the carrier-sensing airtime is obtained by the loop calculation depending on the number of frame lengths existing on the network.

G. IDLE AIRTIME

The idle airtime of Node i is the timeshare of the BT decrement or the absence of a frame in the buffer. Since the node is in the idle, transmission, or carrier-sensing state, the idle airtime, Z_i, is as follows

$$Z_i = 1 - X_i - Y_i. \tag{19}$$

H. THROUGHPUT

When SN i connects to RN j, the end-to-end throughput of SN i, $E_{i,j}$, is

$$E_{i,j} = \begin{cases} \frac{q_{j,i}}{\sum_{k\in\nu(j)} q_{j,k}} \frac{Z_j G_j (1-\gamma_j) P_i}{\sigma} & (q_j = 1) \\ \frac{q_{j,i} Z_j G_j (1-\gamma_j) P_i}{\sigma} & (q_j \neq 1). \end{cases} \tag{20}$$

Because the throughput of RN i is the total throughput of the SNs that connect with RN i, the throughput of RN i is

$$E_i = \sum_{j\in\nu(i)} E_{j,i}. \tag{21}$$

I. END-TO-END DELAY

In the investigated tree-topology network, the end-to-end delay is the sum of the single-hop transmission delay from the SN to the RN and the single-hop transmission delay from the RN to the destination node. The single-hop transmission delay consists of two parts, the Medium Access Control (MAC) access delay and the queuing delay, as shown in Fig. 4.

The MAC access delay contains the transmission, BT-freezing, and BT-decrement durations for the successful transmission of one frame. It is assumed that the frame-existence probability in the carrier-sensing state is the same as that during the entire time. As shown in [26], the frame-existence probability during the entire time, Q_i is

$$Q_i = \frac{X_i + q_i Z_i}{1 - Y_i} = \frac{X_i + q_i Z_i}{X_i + Z_i}, \tag{22}$$

where $\frac{Q_i Y_i + q_i Z_i}{X_i}$ is the total duration of BT-freezing and BT-decrement to the transmission one. The MAC access delay can be derived as

$$\begin{aligned} D_{M_i} &= T_i R_i \left(1 + \frac{Q_i Y_i + q_i Z_i}{X_i}\right) \\ &= \frac{T_i R_i (X_i + q_i Z_i)}{X_i (X_i + Z_i)}. \end{aligned} \tag{23}$$

The queuing delay is the duration from the instant when a frame arrives at Node i to the instant when the frame reaches the top of the buffer. We use the M/M/1 queueing model, hence the frame service rate of Node i, μ_i is

$$\mu_i = \frac{1}{D_{M_i}} = \frac{X_i (X_i + Z_i)}{T_i R_i (X_i + q_i Z_i)}. \tag{24}$$

Therefore, the buffer-utilization rate of Node i, ρ_i, is

$$\begin{aligned} \rho_i &= \frac{\lambda_i}{\mu_i} \\ &= \frac{X_i + q_i Z_i}{X_i + Z_i} \\ &= Q_i. \end{aligned} \tag{25}$$

The probability that Node i has l frames in its buffer is

$$b_{i,l} = \frac{\lambda_i}{\mu_i} b_{i,l-1} = \cdots = \left(\frac{\lambda_i}{\mu_i}\right)^l b_{i,0} = Q_i^l b_{i,0}, \tag{26}$$

where $b_{i,0}$ expresses the probability that Node i has no frame. On the other hand, the sum of all probabilities with different values of l equals 1. If we denote the buffer size as L, we have

$$\sum_{l=0}^{L} b_{i,l} = \frac{1 - Q_i^{L+1}}{1 - Q_i} b_{i,0} = 1. \tag{27}$$

From Eqs. (26) and (27),

$$b_{i,l} = \frac{Q_i^l - Q_i^{l+1}}{1 - Q_i^{L+1}}. \tag{28}$$

Therefore, the queuing delay is

$$\begin{aligned} D_{Q_i} &= \sum_{l=1}^{L} \left[\frac{D_{M_i}}{2} + (l-1) D_{M_i}\right] b_{i,l} \\ &= \frac{1 - 3Q + 3Q^2 - 4(L-1)Q^{L+2} + 2LQ^{L+3}}{2\left(1 - Q^{L+1}\right)(1-Q)^2} \end{aligned} \tag{29}$$

Because the transmission delay of Node i is the sum of the MAC access delay and the queuing delay, the transmission delay is

$$D_i = D_{M_i} + D_{Q_i}. \tag{30}$$

Accordingly, the end-to-end delay from SN i, which connects to RN j, is

$$D_{i,j} = D_{M_i} + D_{Q_i} + D_{M_j} + D_{Q_j}. \tag{31}$$

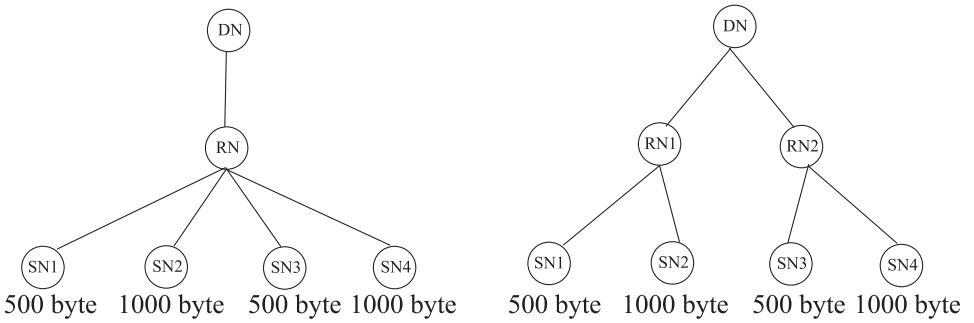

(a) Scenario 1: four SNs connect to one RN

(b) Scenario 2: two RNs, each is the upstream for two SNs

FIGURE 5. Evaluated network topologies.

TABLE 2. System parameters.

MAC header	24 bytes
PHY header	16 bytes
ACK size	10 bytes
DATA payload	100, 500, 1000 bytes
Data rate	54 Mbps
ACK bit rate	24 Mbps
$SIFS$	16 μsec
$DIFS$	34 μsec
slot time (σ)	9 μsec
CW_{min}	15
CW_{max}	1023
Retransmission limit (K)	7
Buffer size (L)	100 frames

IV. EVALUATION

In this section, we first present the validity of the proposed analytical analysis compared to the previous works. Among the airtime-based proposals, the closet ones related to ours are in [26], [31], which are for the end-to-end delay and throughput of string multi-hop IEEE 802.11 network, respectively. We then show the comparisons between the analytical and simulation results for a tree-topology network. Regarding the analytical results of throughput, we consider both the models provided by Eq. (14) and Eq. (16). On the other hand, we use the network simulator, which has been developed by our laboratory, for the evaluations [37]. The investigated tree-topology networks include four source nodes (SNs) and one destination node (DN). The pair SN{1, 3} are configured to generate 500-byte frames, while the other nodes (SN2, 4) generate frames, whose size is 1000 bytes. We consider two scenarios (i.e., Scenario 1, 2), which have different numbers of RN. In Scenario 1, one RN connects to all SNs, as shown in Fig. 5a. Figure 5b illustrates Scenario 2, where SN{1, 2}, {3, 4} connect to RN1, RN2, respectively. In the scenarios, each SN yields frames with an identical offered load. Table 2 gives system parameters used in the evaluations. The parameters are based on the IEEE 802.11a standard.

A. VALIDATION

This research is unique in using the airtime-based and Bianchi model to construct a mathematical expression for the performance of the IEEE 802.11 tree-based network. Therefore, the closely related works are the string topology analysis, since the string topology is considered as the simplest tree. Because our work covers both the throughput and end-to-end delay, we select the two corresponding models of those metrics (i.e., the delay model in [26], and the throughput one in [31]). We compare the model in the string scenario of SN1-RD-DN, as in the leftmost branch in Fig. 5a. For a fair comparison, we investigate the 100-byte and 500-byte packets in this validation. That is because the 100-byte size is among the main evaluation parameters in the previous work.

The throughput validation between our work and [31] is shown in Fig. 6a, which captures the variation of the end-to-end throughput following the offered load. We can reveal the saturation point, as well as the throughput values with both packet sizes. Intuitively, the bigger packet size gives better throughput performance. When the offered load increases, the network also gets to the saturated state later with the bigger ones. In all investigated cases, the results from both models are well matched. Hence, our model can include the model in [31]. We can conclude that our work is more comprehensive than [31] because our throughput model can handle more generalized topologies. Moreover, we can provide the analysis for the end-to-end delay. The validation of our delay model and [26] under the offered load variation is presented in Fig. 6b. First, we can see that the saturation points are agreed between [26], [31], and our models. Second, we can conclude the same conclusion for the relationship between our delay model and [26]. Overall, the through and delay results confirm the validity of our models.

It is also worthy to note that our models can handle the heterogeneous packet sizes from different sources, which have been similarly addressed in [16]. Although we can simplify our model to include [16], we don't conduct the validation. The reason is that the target of [16] is a single-hop WLAN, while ours is the multi-hop tree-based network. Separate from that aspect, we can also have the delay analysis while [16] only has the throughput model.

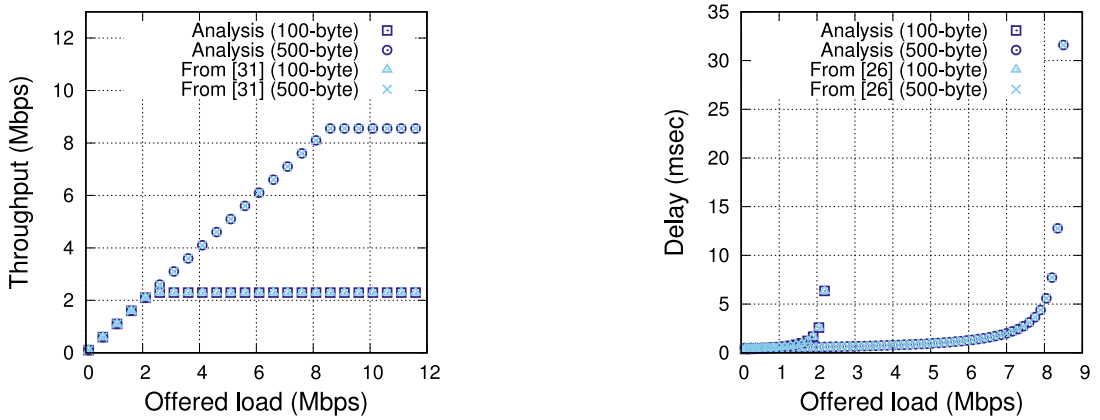

(a) Analytical throughput vs. [31] (b) Analytical delay vs. [26]

FIGURE 6. Validation in a string topology.

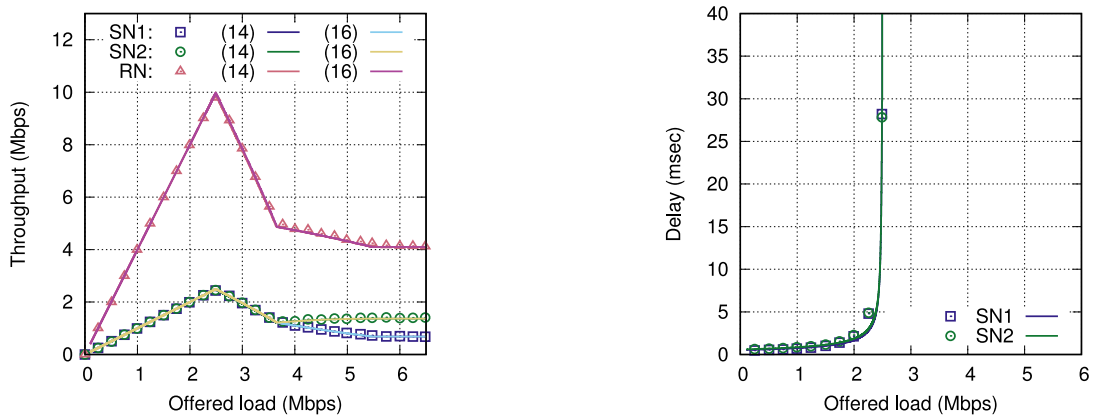

(a) Throughput (b) Delay

FIGURE 7. Performance for each node in Scenario 1 with simulation (points) and analysis (lines); (14), (16) indicate the analytical model in Eqs. (14), (16), respectively.

B. SCENARIO 1

Figure 7 shows a comparison of the analytical and evaluation results in Scenario 1. Figure 7a and Fig. 7b respectively present the throughput, latency performance as a function of the offered load of the SNs, RN. It can be seen from Fig. 7a that the throughput increases in proportion to the offered load (O) in the range of $0 \leq O \leq 2.4$ Mbps. That indicates all the nodes are in the non-saturation state. Because the RN has relayed the frames, which are transmitted from the source nodes, the frame-existence probability of the RN reaches one earliest. In other words, the RN in the first node which turns into the saturation state. Accordingly, the throughput of RN becomes the maximum when $O = 2.4$ Mbps. When O becomes larger than 2.4 Mbps, the throughput values of all nodes decrease. Note that SN1's packet size is smaller than SN2' one; and the nodes share the identical offered load condition. Therefore, the frame generation probability of SN1 increases faster than the one of SN2. Consequently, the frame-existence probability of SN1 reaches one before that of SN2 does. Later, when SN2's frame-existence probability also becomes one, all the nodes fall into the saturated condition. On the other hand, we can observe the delay variation in Fig. 7b, where each SN's delay significantly increases just before the frame-existence probability of the RN reaches one (i.e., the RN being saturated). After the RN is in the saturation state, the delay becomes infinite.

From Fig. 7, the analytical predictions agree with the simulation results quantitatively, showing that the analytical model is valid for the tree-topology network with one RN. In addition, the analytical predictions using Eq. (14) and Eq. (16) are perfectly matched. This means that the analytical model using Eq. (16) achieves both low calculation cost and accuracy of analytical prediction.

C. SCENARIO 2

Figure 8 shows the throughput and the delay performance as a function of the offered load in Scenario 2. Similarly to the throughput result of Scenario 1, Fig. 8a shows the proportional increment of the RNs, SNs' throughput when the offered load increases before the saturation point. When the frame-existence probabilities of the RNs become one, their throughput values are maximum. After the RNs are in the saturated condition, the throughput of each network node decreases. Because of the packet size, the frame-existence

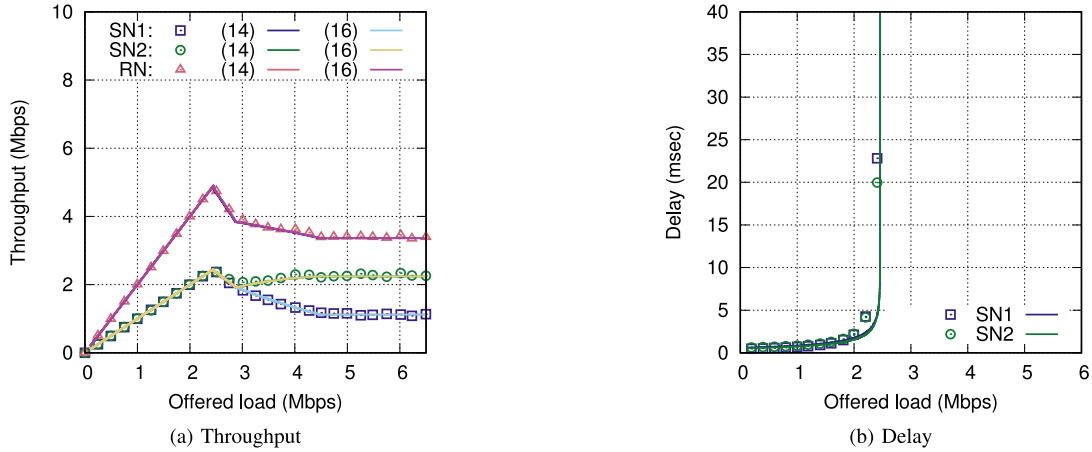

(a) Throughput (b) Delay

FIGURE 8. Performance for each node in Scenario 2 with simulation (points) and analysis (lines); (14), (16) indicate the analytical model in Eqs. (14), (16), respectively.

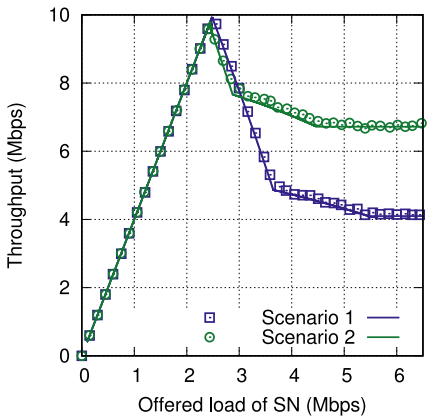

FIGURE 9. Comparing network throughput in Scenario 1 and Scenario 2 with simulation (points) and analysis (lines).

probability of SN2 reaches one last. After that, all nodes will have their saturated throughput values. Figure 8b presents the delay of the frame generated from the SNs in Scenario 2. Before the point of network saturation, the delay increases following the offered load with a similar performance as in Scenario 1. The similarity continues when the frame-existence probability of the RNs become one.

Once again, from the results in Fig. 8, we can conclude the good agreement between the analytical and simulation results. That confirms the applicability of our model for the tree-topology network with multiple RNs. Besides, we also got the perfect match between the prediction using Eq. (14) and Eq. (16). It suggests the investigated scenario is not challenging enough in the computation for Eq. (14), hence it is worthy of investigating furthermore.

D. COMPARISON BETWEEN SCENARIO 1 AND SCENARIO 2

Figure 9 shows the comparison of network throughput in Scenario 1 and 2. We can see that when the offered load increases from 0, because of the increasing throughput of SNs, RNs, the network throughput behaves in the same manner until the saturation point. Within this period, the two networks share identical throughput performance. When the RNs turn into the saturation state, both reach the maximum network throughput. After that, when the frame-existence probabilities of all the network nodes are one, the network is saturated. In such a condition, the saturated network throughput of Scenario 2 is higher than that of Scenario 1. That is because four SNs send data to the destination via an RN in Scenario 1, whereas in Scenario 2, two nodes share an RN. Note that, in Scenario 2, the two RNs forward the data frame to the same destination. As a result, the two RNs can relay more loads, then let the network throughput in Scenario 2 be better. Another interesting observation is that the network in Scenario 2 reaches the network saturation point earlier than the one in Scenario 1.

V. CONCLUSION AND FUTURE WORK

This article has presented analytical expressions of delay and throughput for the IEEE 802.11-based tree-topology network at any offered load. We observe that concurrent transmissions mainly cause the frame collisions because the nodes can sense the other's communication. To tackle the challenge, the proposed model incorporated relay-node operations into a WLAN analysis with the airtime concept. Specifically, this work adopts a Bianchi model-based analysis for expressing the frame collision probability caused by concurrent transmission. Besides, utilizing the airtime-based analysis, the ratio of frame numbers of each flow in an RN was revealed. The presented analytical model consequently obtained the network throughput, the throughput, and the delay of each flow. The simulation results have confirmed the validity of the analytical expressions. Both the results are well-matched with each other.

In the future, we plan to explore the analytical models in more complicated tree scenarios (e.g., with more nodes, more layers) and take into account the features and parameters of other IEEE 802.11 standards. We also investigate the

condition where the calculation cost in Eq. (16) is more beneficial than the one in Eq. (14).

REFERENCES

[1] E. C. Eze, S.-J. Zhang, E.-J. Liu, and J. C. Eze, "Advances in vehicular ad-hoc networks (VANETs): Challenges and road-map for future development," *Int. J. Autom. Comput.*, vol. 13, no. 1, pp. 1–18, Feb. 2016.

[2] B. Masini, A. Bazzi, and A. Zanella, "A survey on the roadmap to mandate on board connectivity and enable V2V-based vehicular sensor networks," *Sensors*, vol. 18, no. 7, p. 2207, Jul. 2018.

[3] C. Huang, M. Chiang, D. Dao, W. Su, S. Xu, and H. Zhou, "V2V data offloading for cellular network based on the software defined network (SDN) inside mobile edge computing (MEC) architecture," *IEEE Access*, vol. 6, pp. 17741–17755, 2018.

[4] N. K. Suryadevara and S. C. Mukhopadhyay, "Wireless sensor network based home monitoring system for wellness determination of elderly," *IEEE Sensors J.*, vol. 12, no. 6, pp. 1965–1972, Jun. 2012.

[5] S. D. T. Kelly, N. K. Suryadevara, and S. C. Mukhopadhyay, "Towards the implementation of IoT for environmental condition monitoring in homes," *IEEE Sensors J.*, vol. 13, no. 10, pp. 3846–3853, Oct. 2013.

[6] Q. T. Minh, K. Nguyen, C. Borcea, and S. Yamada, "On-the-fly establishment of multihop wireless access networks for disaster recovery," *IEEE Commun. Mag.*, vol. 52, no. 10, pp. 60–66, Oct. 2014.

[7] K. Ali, H. X. Nguyen, Q. Vien, P. Shah, and Z. Chu, "Disaster management using D2D communication with power transfer and clustering techniques," *IEEE Access*, vol. 6, pp. 14643–14654, 2018.

[8] A. M. Hayajneh, S. A. R. Zaidi, D. C. McLernon, M. Di Renzo, and M. Ghogho, "Performance analysis of UAV enabled disaster recovery networks: A stochastic geometric framework based on cluster processes," *IEEE Access*, vol. 6, pp. 26215–26230, 2018.

[9] J. Gutiérrez, J. F. Villa-Medina, A. Nieto-Garibay, and M. Á. Porta-Gándara, "Automated irrigation system using a wireless sensor network and GPRS module," *IEEE Trans. Instrum. Meas.*, vol. 63, no. 1, pp. 166–176, Jan. 2014.

[10] G. Bianchi, "Performance analysis of the IEEE 802.11 distributed coordination function," *IEEE J. Sel. Areas. Commun.*, vol. 18, no. 3, pp. 535–547, Mar. 2000.

[11] A. Kumar, E. Altman, D. Miorandi, and M. Goyal, "New insights from a fixed-point analysis of single cell IEEE 802.11 WLANs," *IEEE/ACM Trans. Netw.*, vol. 15, no. 3, pp. 588–601, Jun. 2007.

[12] K. Duffy, D. Malone, and D. J. Leith, "Modeling the 802.11 distributed coordination function in non-saturated conditions," *IEEE Commun. Lett.*, vol. 9, no. 8, pp. 715–717, Aug. 2005.

[13] D. Malone, K. Duffy, and D. Leith, "Modeling the 802.11 distributed coordination function in nonsaturated heterogeneous conditions," *IEEE/ACM Trans. Netw.*, vol. 15, no. 1, pp. 159–172, Feb. 2007.

[14] P. Chatzimisios, A. C. Boucouvalas, and V. Vitsas, "Effectiveness of RTS/CTS handshake in IEEE 802.11a wireless LANs," *Electron. Lett.*, vol. 40, no. 14, pp. 915–916, Jul. 2004.

[15] Y. Gu, Q. Cui, Y. Chen, W. Ni, X. Tao, and P. Zhang, "Effective capacity analysis in ultra-dense wireless networks with random interference," *IEEE Access*, vol. 6, pp. 19499–19508, 2018.

[16] Y. Wan *et al.*, "Throughput analysis of WLANs in saturation and non-saturation heterogeneous conditions with airtime concept," *IEICE Trans. Commun.*, vol. E99.B, no. 11, pp. 2289–2296, Nov. 2016.

[17] S. Ikuma, Z. Li, T. Pei, Y.-J. Choi, and H. Sekiya, "Rigorous analytical model of saturated throughput for the IEEE 802.11p EDCA," *IEICE Trans. Commun.*, vol. E102-B, no. 4, pp. 699–707, 2019.

[18] P. C. Ng and S. C. Liew, "Throughput analysis of IEEE802.11 multi-hop ad hoc networks," *IEEE/ACM Trans. Netw.*, vol. 15, no. 2, pp. 309–322, Apr. 2007.

[19] Y. Gao, D.-M. Chiu, and J. C. S. Lui, "Determining the end-to-end throughput capacity in multi-hop networks: Methodology and applications," in *Proc. ACM SIGMETRICS/Perform.*, 2006, pp. 39–50.

[20] Y. Barowski, S. Biaz, and P. Agrawal, "Towards the performance analysis of IEEE 802.11 in multi-hop ad-hoc networks," in *Proc. IEEE WCNC*, 2005, pp. 100–106.

[21] M. Noor-A-Rahim, G. G. M. N. Ali, H. Nguyen, and Y. L. Guan, "Performance analysis of IEEE 802.11p safety message broadcast with and without relaying at road intersection," *IEEE Access*, vol. 6, pp. 23786–23799, 2018.

[22] M. Inaba, Y. Tsuchiya, S. Sakata, and K. Yagyu, "Analysis and experiments of maximum throughput in wireless multi-hop networks for VoIP application," *IEICE Trans. Commun.*, vol. 92-B, no. 11, pp. 3422–3431, Nov. 2009.

[23] T. Sugimoto, N. Komuro, H. Sekiya, S. Sakata, and K. Yagyu, "Maximum throughput analysis for RTS/CTS-used IEEE 802.11 DCF in wireless multi-hop networks," in *Proc. Int. Conf. Comput. Commun. Eng. (ICCCE)*, 2010, pp. 1–6.

[24] H. Sekiya, Y. Tsuchiya, N. Komuro, and S. Sakata, "Analytical expressions of maximum throughput for long-frame communications in one-way string wireless multihop networks," in *Proc. Int. Conf. Ubiquitous Future Netw. (ICUFN)*, 2010, pp. 121–126.

[25] K. Sanada, H. Sekiya, N. Komuro, and S. Sakata, "Backoff-stage synchronization in three-hop string-topology wireless networks with hidden nodes," *Nonlinear Theory Appl. IEICE*, vol. 3, no. 2, pp. 200–214, 2012.

[26] K. Sanada, J. Shi, N. Komuro, and H. Sekiya, "End-to-end delay analysis for IEEE 802.11 string-topology multi-hop networks," *IEICE Trans. Commun.*, vol. E98.B, no. 7, pp. 1284–1293, 2015.

[27] Y. Shimoyamada, K. Sanada, N. Komuro, and H. Sekiya, "End-to-end throughput analysis for IEEE 802.11e EDCA string-topology wireless multi-hop networks," *Nonlinear Theory Appl. IEICE*, vol. 6, no. 3, pp. 410–432, 2015.

[28] D. Vassis and G. Kormentzas, "Performance analysis of IEEE 802.11 ad hoc networks in the presence of exposed terminals," *Ad Hoc Netw.*, vol. 6, pp. 474–482, May 2008.

[29] H. Zhao, E. Garcia-Palacios, S. Wang, J. Wei, and D. Ma, "Evaluating the impact of network density, hidden nodes and capture effect for throughput guarantee in multi-hop wireless networks," *Ad Hoc Netw.*, vol. 11, no. 1, pp. 54–69, 2013.

[30] N. Komuro *et al.*, "Design and analysis of multi-channel mac protocol with channel grouping in wireless ad-hoc networks," *IEICE Trans. Commun.*, vol. E99.B, pp. 2305–2314, Nov. 2016.

[31] K. Sanada, N. Komuro, Z. Li, T. Pei, Y.-J. Choi, and H. Sekiya, "Generalized analytical expressions for end-to-end throughput of IEEE 802.11 string-topology multi-hop networks," *Ad Hoc Netw.*, vol. 7, pp. 135–148, Mar. 2018.

[32] T. Kanematsu, K. Nguyen, and H. Sekiya, "Throughput analysis for IEEE 802.11 multi-hop networks considering transmission rate," in *Proc. IEEE VTC Spring*, 2019, pp. 1–5.

[33] M. Yazid and A. Ksentini, "Modeling and performance analysis of the main MAC and PHY features of the 802.11ac standard: A-MPDU aggregation vs spatial multiplexing," *IEEE Trans. Veh. Technol.*, vol. 67, no. 11, pp. 10243–10257, Nov. 2018.

[34] T. Kanematsu *et al.*, "Analytical evaluation of a WLAN with dense network nodes considering capture effect," *IEICE Trans. Commun.*, vol. E103-B, no. 7, pp. 815–825, 2020.

[35] J. Liu *et al.*, "Throughput analysis of IEEE 802.11 WLANs with inter-network interference," *Appl. Sci.*, vol. 10, no. 6, p. 2192, Mar. 2020.

[36] R. Laufer and L. Kleinrock, "On the capacity of wireless CSMA/CA multihop networks," in *Proc. IEEE INFOCOM*, 2013, pp. 1312–1320.

[37] *802.11 Simulator*. Accessed: May 2020. [Online]. Available: http://www.s-lab.nd.chiba-u.jp/files/

TAKESHI KANEMATSU (Member, IEEE) was born in Tokyo, Japan, in August 17, 1995. He received the B.E. degree from Chiba University, Japan, in 2018. His research interests include throughput analysis and simulation for IEEE 802.11 in wireless networks.

YIN WAN was born in Jiansu, China, in October 28, 1990. He received the B.E. degree from the Nanjing University of Posts and Telecommunications, China, in 2013, and the M.E. degree from Chiba University, Japan, in 2016. His research interests include throughput analysis and simulation for IEEE 802.11 in wireless multihop networks.

KOSUKE SANADA (Member, IEEE) was born in Hokkaido, Japan, in October 20, 1987. He received the B.E., M.E., and Ph.D. degrees from Chiba University, Japan, in 2011, 2012, and 2015, respectively. From October 2015 to February 2016, he was a Postdoctoral Researcher with the Chiba University. Since March 2016, he has been with Mie University, Mie, Japan, where he is currently working as an Assistant Professor. His research interests include mathematical analysis, and simulation and experiment for IEEE 802.11 in wireless multihop networks.

ZHETAO LI (Member, IEEE) received the B.Eng. degree in electrical information engineering from Xiangtan University in 2002, the M.Eng. degree in pattern recognition and intelligent system from Beihang University in 2005, and the Ph.D. degree in computer application technology from Hunan University in 2010. He was a Visiting Researcher with Ajou University from May to August 2012. From December 2013 to December 2014, he was a Postdoctoral Researcher in wireless network with Stony Brook University. From December 2014 to March 2015, he was a Visiting Professor with Ajou University.

TINGRUI PEI received the B.E. and M.E. degrees from Xiangtan University, Hunan, China, in 1992 and 1998, respectively, and the Doctoral degree in signal and information processing from the Beijing University of Posts and Telecommunications in June 2004. He visited Waseda University, Japan, as a Researcher from February 2006 to February 2007. He is currently a Professor with Xiangtan University.

YOUNG-JUNE CHOI (Senior Member, IEEE) received the B.S., M.S., and Ph.D. degrees from the Department of Electrical Engineering and Computer Science, Seoul National University, South Korea, in 2000, 2002, and 2006, respectively. From September 2006 to July 2007, he was a Postdoctoral Researcher with the University of Michigan, Ann Arbor, MI, USA. From 2007 to 2009, he was with NEC Laboratories America, Princeton, NJ, USA, as a Research Staff Member. He joined Ajou University as a Faculty Member in September 2009.

KIEN NGUYEN (Senior Member, IEEE) received the B.E. degree in electronics and telecommunication from the Hanoi University of Science and Technology, Vietnam, in 2004, and the Ph.D. degree in informatics from the Graduate University for Advanced Studies, Japan, in 2012. He is currently an Assistant Professor with the Graduate School of Science and Engineering, Chiba University. He has published more than 90 publications in peer-reviewed journals and conferences and two patents. His research covers a wide range of topics, including the Internet, Internet of Things technologies, and wired and wireless communication. He is a member of IEICE. He also is involved in IETF activities.

HIROO SEKIYA (Senior Member, IEEE) was born in Tokyo, Japan, in July 1973. He received the B.E., M.E., and Ph.D. degrees in electrical engineering from Keio University, Yokohama, Japan, in 1996, 1998, and 2001, respectively. Since April 2001, he has been with Chiba University, Chiba, Japan, where he is currently a Professor with the Graduate School of Science and Engineering. His research interests include high-frequency high-efficiency tuned power amplifiers, resonant dc/dc power converters, dc/ac inverters, and digital signal processing for wireless communications. He is a Senior Member of the Institute of Electronics, Information and Communication Engineers, Japan, and a member of Institute of Electronics, Information Processing Society of Japan, and the Research Institute of Signal Processing, Japan.